Ocean Engineering 120 (2016) 383–388

Contents lists available at ScienceDirect

Ocean Engineering

journal homepage: www.elsevier.com/locate/oceaneng

Numerical assessment of cargo liquefaction potential

Lei Ju, Dracos Vassalos, Evangelos Boulougouris

Ship Stability Research Centre, Department of Naval Architecture, Ocean & Marine Engineering, University of Strathclyde, 100 Montrose Street, Glasgow G4 0LZ, Scotland, UK

ARTICLE INFO

Article history:
Received 20 November 2015
Accepted 16 January 2016
Available online 3 February 2016

Keywords:
Cargo liquefaction
UBC3D-PLM modelling
Ship stability

ABSTRACT

Liquefaction of fine particle cargoes, resulting in cargo shift and loss of stability of ships, has caused the loss of many lives in marine casualties over the recent past years. Since the dangers of cargo liquefaction have long been known to the shipping industry, the question of why the phenomenon is resurfacing now would be a legitimate one. With this in mind, an UBC3D-PLM model based on FEM theory in the commercial software PLAXIS is presented in this paper as a means to consider soil DSS (Direct Simple Shear) test to verify the model and a method is presented to assess cargo liquefaction potential. Shaking table tests with different amplitude, frequency and initial degree of saturation of cargoes are studied to predict time-domain characteristics. The proposed method could be used as a reference in support of a suitable regulatory framework to address liquefaction and its effect on ship stability.

1. Introduction

Liquefaction of mineral ores, such as ore fines from India and nickel ore from Indonesia, the Philippines and New Caledonia, resulting in cargo shift and loss of ship stability, has been a major cause of marine casualties over the past few years. Such a transition during ocean carriage can cause a sudden loss of stability of the carrying vessel. While cargoes are loaded on board a vessel, the material is exposed to mechanical agitation and energy input in the form of engine vibrations, vessel motions and wave impact, resulting in a gradual settling and compaction of the cargo. The gaps between the particles become smaller in the process with the corresponding pore pressure progressively increasing. As a result, the water holding ability or matric suction of particles decreases and the water in the interstellar spaces comes together to form a liquid layer that allows the cargo above to move relative to the cargo below as if the two layers were part of a liquid, hence the term liquefaction. Alternative outcomes include the formation of a wet base that may lead to shift of the whole cargo above and the potential loss of the vessel or the formation of free surface comprising heavy “slurry” that could lead to structural damage of the outer shell or internal bulkheads and/or loss of stability again.

The UBC3D-PLM model is a powerful constitutive model, which is a 3-D extension of the UBCSAND model introduced by Beaty and Byrne (1998). The Mohr–Coulomb yield condition in a 3-D principal stress space is used. The bulk modulus of water is depended upon the degree of saturation, which is specified via PLAXIS input, enabling the prediction of the pore pressure evolution in unsaturated particles.

2. Key features of UBC3D-PLM

2.1. Yield surface

Mohr–Coulomb yield function generalised in 3-D principal stress space is used in UBC3D-PLM model (Alexandros and Galavi, 2013) as presented in Fig. 1.

The critical yield surface could be defined as given by Eq. (1):

$$f_m = \frac{\sigma'_{max} - \sigma'_{min}}{2} - \left(\frac{\sigma'_{max} + \sigma'_{min}}{2} + c' \cot \varphi'_p\right) \sin \varphi_{mob} \tag{1}$$

where, σ'_{max} and σ'_{min} are the maximum and minimum principal stresses respectively, c' is the cohesion of the soil, ϕ'_p is the peak friction angle of the soil and ϕ_{mob} is the mobilised friction angle during hardening.

2.2. Elasto-plastic behaviour

The elastic behaviour, which occurs within the yield surface is controlled by two parameters expressed in terms of the elastic bulk modulus K^e_B and the elastic shear modulus K^e_G as shown below:

$$K^e_B = k^e_B P_A \left(\frac{p'}{P_A}\right)^{me} \tag{2}$$

$$K^e_G = k^e_G P_A \left(\frac{p'}{P_A}\right)^{ne} \tag{3}$$

where, p' is the mean effective stress, P_A is the reference stress (usually equal to 100 kPa), k^e_B and k^e_G are the bulk and shear

http://dx.doi.org/10.1016/j.oceaneng.2016.01.024
0029-8018/

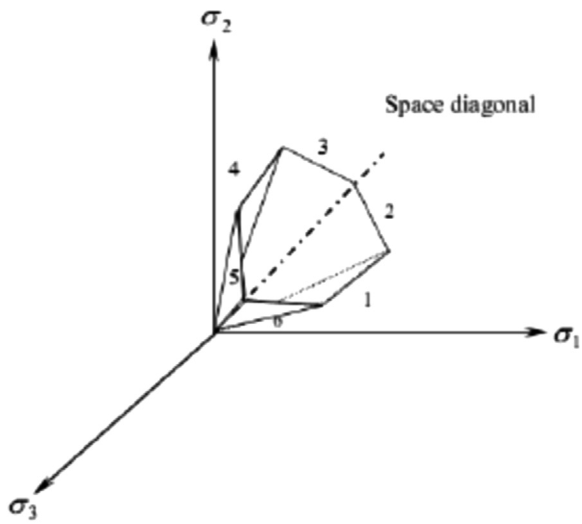

Fig. 1. Mohr–Coulomb yield surface in principal stress space.

modulus numbers respectively and, me and ne are the elastic exponents which define the rate dependency of stiffness.

The hardening rule as reformulated by Tsegaye (2011) in UBC3D-PLM model is given as:

$$d\ \sin\ \phi_{mob} = 1.5K_G^p\left(\frac{p}{P_A}\right)^{np}\frac{P_A}{P_m}\left(1-\frac{\sin\ \phi_{mob}}{\sin\ \phi_{peak}}R_f\right)^2 d\lambda \tag{4}$$

where, $d\lambda$ is the plastic strain increment multiplier, np is the plastic shear modulus exponent, ϕ_{mob} is the mobilised friction angle, which is defined by the stress ratio, ϕ_{peak} is the peak friction angle and R_f is the failure ratio n_f/n_{ult}, ranging from 0.5 to 1.0.

2.3. Cyclic mobility

This behaviour is presented in Fig. 2 picturing the process of cyclic mobility of dense sand. The stiffness degradation is computed as follows:

$$K_G^p = K_{G,primary}^p * e^{E_{dil}} \tag{5}$$

$$E_{dil} = \min(110^{*}\varepsilon_{dil}, fac_{post}) \tag{6}$$

where ε_{dil} is accumulation of the plastic deviatoric strain, which is generated during dilation of the soil element and the input parameter fac_{post} is the value of the exponential multiplier term.

2.4. Undrained behaviour

The increment of the pore water pressure is computed by the following equation:

$$dp_w = \frac{K_w}{n} d\varepsilon_v \tag{7}$$

where, K_w is the bulk modulus of the water, n is the soil porosity and $d\varepsilon_v$ is the volumetric strain of the fluid.

The bulk modulus of water is dependent upon the degree of saturation of the soil. The bulk modulus of the unsaturated water is defined as follows:

$$K_w^{unsat} = \frac{K_w^{sat} K_{air}}{SK_{air} + (1-S)K_w^{sat}} \tag{8}$$

where K_w^{sat} is the bulk modulus of the saturated water and K_{air} is the bulk modulus of air, which equals 1 kPa in this implementation having the minimum value that allows avoiding the generation of pore pressures during modelling dry sand S is the degree of saturation.

3. Validation of the UBC3D-PLM in element test

3.1. Validation of the UBC3D-PLM in monotonic loading

The validation of the UBC3D-PLM in monotonic loading is presented in this section. The input parameters for modelling the tri-axial compression test (TxC) and the direct simple shear test (DSS) on loose Syncrude sand are given in Table 1. The results of the UBC3D-PLM are in a good agreement with the experimental data (Puebla et al., 1997) as shown in Fig. 3.

3.2. Validation of the UBC3D-PLM in cyclic loading

The behaviour of loose Fraser sand under cyclic direct simple shear is modelled and the numerical results are compared with experimental data as published by Sriskandakumar (2004). The relative density (RD) of the tested sand is 40%. In Fig. 4, the evolution of stress–strain is presented. The applied CSR equals 0.08. The vertical applied stress is 100 kPa. The K0 factor is assumed to be 1 for simplification.

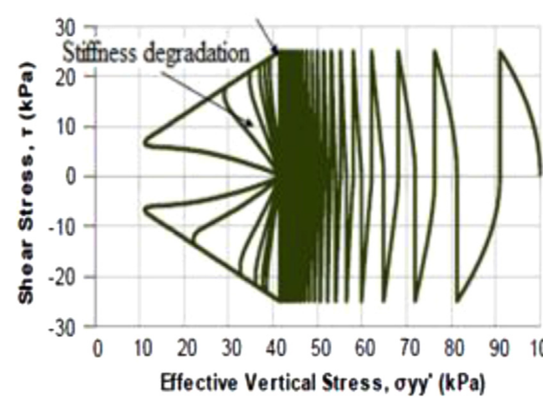

Fig. 2. Undrained cyclic shear stress path reproduced with UBC3D-PLM for dense sand. Cyclic mobility, stiffness degradation and soil densification are referenced on the graph.

Table 1
UBC3D input parameters for all the validation tests.

Parameter	Syncrude S. (TxC, DSS)	Fraser S. (Cyclic DSS)	Cargo (FEM)
$\varphi_p(\circ)$	33.7	33.8	31.2
$\varphi_{cv}(\circ)$	33	33	34.6
k_B^e	300	607	720
k_G^e	300	867	1031
$K_G^p(TxC)$	310	–	
$K_G^p(DSS)$	98.3	266	700
$me = ne$	0.5	0.5	0.5
np	0.5	0.4	0.4
R_f	0.95	0.81	0.74
$N1(60)$	8	8	13
fac_{hard}	1	1	0.45
fac_{post}	0	0.6	0.01